

Large Angle Hadron Correlations from Medium-Induced Gluon Radiation

Ivan Vitev

Los Alamos National Laboratory, Theory Division and Physics Division, Mail Stop H846,
Los Alamos, NM 87544

E-mail: ivitev@lanl.gov

Abstract. Final state medium-induced gluon radiation in ultradense nuclear matter is shown to favor large angle emission when compared to vacuum bremsstrahlung due to the suppression of collinear gluons. In a simple model of momentum transfers from the medium to the jet+gluon system the phase space distribution of non-Abelian bremsstrahlung is examined to first order in opacity. Perturbative expression for the contribution of the hadronic fragments from medium-induced gluons to the back-to-back particle correlations is derived. It is found that in the limit of large jet energy loss gluon radiation determines the yield and angular distribution of $|\Delta\varphi| \geq \frac{\pi}{2}$ di-hadrons to high transverse momenta p_{T_2} of the associated particles. Clear transition from enhancement to suppression of the away-side di-hadron correlations is established at moderate p_{T_2} and its experimentally accessible features are predicted versus the trigger particle momentum p_{T_1} . The measured away-side correlation function is shown to be sensitive to the broad rapidity distribution of di-jets and their vacuum and medium-induced acoplanarity.

1. Introduction

The discovery of jet quenching [1] – the suppression of large transverse momentum hadron production in nuclear collisions relative to the expectation from p+p reactions scaled by the number of elementary nucleon-nucleon interactions – is arguably the most exciting new result from the Au+Au experimental program at the Relativistic Heavy Ion Collider (RHIC). The phenomenon of jet quenching has been established via the attenuation of the single inclusive particle spectra [2] and the suppression of the back-to-back di-hadron correlations [3, 4]. It has been interpreted as critical evidence for large parton energy loss [5, 6, 7] in ultradense quark-gluon plasma (QGP) – the deconfined state of matter predicted by quantum chromodynamics (QCD).

So far, the observable effects of the medium-induced gluon radiation *itself* were considered to be modest. For tagged jets, assuming thermalization of the lost energy calculated in [8], transport models predicted an increase in the multiplicity of associated particles limited to $p_{T_2} \leq 500$ MeV [9]. Using the angular gluon distribution from [10], jet cone broadening was found to be $< 10\%$ and challenging to detect experimentally even at the CERN Large Hadron Collider (LHC) [11].

In these proceedings we follow Ref. [12] and demonstrate that a mechanism, based on the destructive interference of color currents from hard and soft parton scattering, can ensure broad in angle and frequency final state medium-induced emission spectrum in QCD. For large energy loss, perturbative fragmentation of the radiative gluons is found to give a dominant

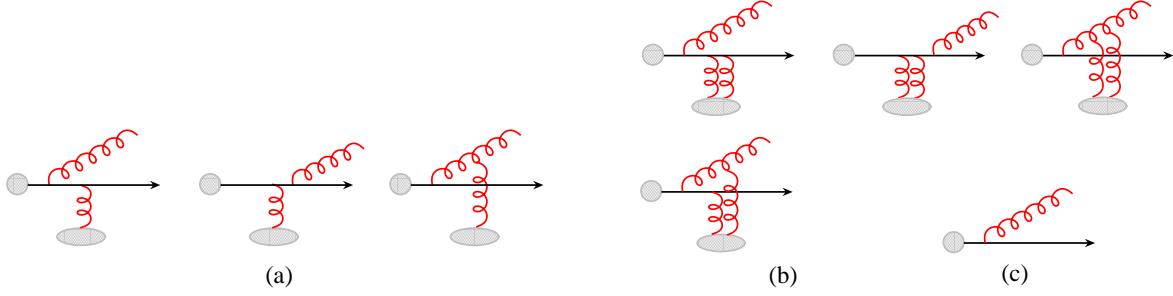


Figure 1. (a) Direct diagrams that contribute to first order in opacity $\bar{n} = L/\lambda$. (b) Double Born diagrams that interfere with the vacuum bremsstrahlung (c) to the same order in \bar{n} .

contribution to the yield of away-side di-hadrons and to significantly alter their correlations at transverse momenta much higher than naively anticipated. We note that the medium-modified jet topology can be distorted in two particle back-to-back measurements by the broad di-jet rapidity distribution and the vacuum and medium-induced acoplanarity. If present, it should be more cleanly detectable on an event-by-event basis and through jet energy flow measurements.

2. Angular distribution of the medium-induced non-Abelian bremsstrahlung

We first recall that for hard perturbative scattering the radiative spectrum of real gluon emission for small and moderate frequencies ω is given by [8]

$$|\mathcal{M}_c|^2 \propto \frac{dN_{\text{vac}}^g}{d\omega d\sin\theta^* d\delta} \approx \frac{C_R \alpha_s}{\pi^2} \frac{1}{\omega \sin\theta^*}. \quad (1)$$

The distribution in Eq. (1) corresponds to the diagram in Fig. 1c where the blob represents the large virtual momentum exchange. In Eq. (1) $\theta^* = \arcsin(k_\perp/\omega)$ is the angle relative to the jet axis, δ is the azimuthal cone angle (both illustrated in Fig. 2), α_s is the strong coupling constant and $C_R = 3(4/3)$ for gluon (quark) jets, respectively. Virtual gluon corrections remove the $\omega \rightarrow 0$ infrared singularity in the cross sections in accord with the Kinoshita-Lee-Nauenberg theorem [13] but the collinear $\theta^* \rightarrow 0$ divergence has to be regulated or subtracted in the parton distribution functions (PDFs) and the fragmentation functions (FFs).

In contrast, the final state medium-induced bremsstrahlung spectrum is both collinear and infrared safe. The full solution for the medium induced gluon radiation off jets produced in a hard collisions at early times $\tau_{jet} \simeq 1/E$ inside a nuclear medium of length L can be obtained to all orders in the correlations between the multiple scattering centers via the reaction operator approach [8]

$$\begin{aligned} \frac{dN_{\text{med}}^g}{d\omega d\sin\theta^* d\delta} &= \sum_{n=1}^{\infty} \frac{dN_{\text{med}}^{g(n)}}{d\omega d\sin\theta^* d\delta} = \omega \sin\theta^* \sum_{n=1}^{\infty} \frac{2C_R \alpha_s}{\pi^2} \prod_{i=1}^n \int_0^{L - \sum_{a=1}^{i-1} \Delta z_a} \frac{d\Delta z_i}{\lambda_g(i)} \\ &\times \int d^2 \mathbf{q}_i \left[\sigma_{el}^{-1}(i) \frac{d\sigma_{el}(i)}{d^2 \mathbf{q}_i} - \delta^2(\mathbf{q}_i) \right] \left(-\mathbf{C}_{(1,\dots,n)} \cdot \sum_{m=1}^n \mathbf{B}_{(m+1,\dots,n)(m,\dots,n)} \right. \\ &\times \left. \left[\cos \left(\sum_{k=2}^m \omega_{(k,\dots,n)} \Delta z_k \right) - \cos \left(\sum_{k=1}^m \omega_{(k,\dots,n)} \Delta z_k \right) \right] \right), \end{aligned} \quad (2)$$

where $\sum_2^1 \equiv 0$ is understood. All vectors in Eq. (2) are two dimensional and coincident with the plane orthogonal to the direction of jet propagation. We denote by $\hat{\delta}$ the unit vector in

the direction of the radiative gluon's transverse momentum, $\mathbf{k} = \omega \sin \theta^* \hat{\delta}$. The color current propagators read

$$\begin{aligned}\mathbf{C}_{(m,\dots,n)} &= \frac{1}{2} \nabla_{\omega \sin \theta^* \hat{\delta}} \ln (\omega \sin \theta^* \hat{\delta} - \mathbf{q}_m - \dots - \mathbf{q}_n)^2, \\ \mathbf{B}_{(m+1,\dots,n)(m,\dots,n)} &= \mathbf{C}_{(m+1,\dots,n)} - \mathbf{C}_{(m,\dots,n)}.\end{aligned}\quad (3)$$

The momentum transfers \mathbf{q}_i are distributed according to a normalized elastic differential cross section

$$\sigma_{el}(i)^{-1} \frac{d\sigma_{el}(i)}{d^2\mathbf{q}_i} = \frac{\mu^2(i)}{\pi(\mathbf{q}_i^2 + \mu^2(i))^2}, \quad (4)$$

which models scattering by soft partons with a thermally generated Debye screening mass $\mu(i)$. From Eq. (4) $\langle \mathbf{q}_i^2 \rangle \propto \mu^2(z_i)$ and for a quark-gluon plasma in local thermal equilibrium $\mu^2(z_i) \sim 4\pi\alpha_s T^2(z_i)$. It has been shown [8] via the cancellation of direct and virtual diagrams that in the eikonal limit only the gluon mean free path $\lambda_g(i)$ enters the medium-induced bremsstrahlung spectrum in Eq. (2). For gluon dominated bulk soft matter $\sigma_{el}(i) \approx \frac{9}{2}\pi\alpha_s^2/\mu^2(i)$ and $\lambda_g(i) = 1/\sigma_{el}(i)\rho(i)$. For the case of (1+1)D dynamical Bjorken expansion of the QGP [5, 6]

$$\mu(z_i) = \mu(z_0) \left(\frac{z_0}{z_i} \right)^{1/3}, \quad \lambda_g(z_i) = \lambda_g(z_0) \left(\frac{z_i}{z_0} \right)^{1/3}. \quad (5)$$

The characteristic path length dependence, $\propto L^2$ for static plasmas, of the non-Abelian energy loss in Eq. (2) comes from the interference phases and is differentially controlled by the inverse formation times,

$$\omega_{(m,\dots,n)} = \frac{(\omega \sin \theta^* \hat{\delta} - \mathbf{q}_m - \dots - \mathbf{q}_n)^2}{2\omega}, \quad (6)$$

and the separations of the subsequent scattering centers $\Delta z_k = z_k - z_{k-1}$. It is the non-Abelian analogue of the Landau-Pomeranchuk-Migdal destructive interference effect in QED [14]. The extension to the case of massive quarks can be carried out systematically to all orders in opacity [15] by identifying the heavy quark mass terms $\propto \omega^2 M_q^2/E^2$.

It can be shown from Eq. (2) that the propagator poles, Eq. (3), where potential divergences may arise are precisely canceled by the interference phases, Eq. (6), to all orders in opacity. This point will be better illustrated if we examine the Gyulassy-Levai-Vitev [8] (GLV) gluon distribution in angle and frequency to first order in the mean number of soft interactions in the plasma. The diagrams shown in Fig. 1 yield:

$$\begin{aligned}|\mathcal{M}_a|^2 + 2\text{Re}\mathcal{M}_b^\dagger \mathcal{M}_c &\propto \frac{dN_{\text{med}}^{g(1)}}{d\omega d\sin\theta^* d\delta} = \frac{2C_R\alpha_s}{\pi^2} \int_{z_0}^L \frac{d\Delta z_1}{\lambda_g(z_1)} \int d^2\mathbf{q}_1 \frac{1}{\sigma_{el}} \frac{d\sigma_{el}}{d^2\mathbf{q}_1}(z_1) \\ &\times \frac{\mathbf{q}_1 \cdot \hat{\delta}}{\mathbf{q}_1^2 - 2\omega \sin \theta^* \mathbf{q}_1 \cdot \hat{\delta} + \omega^2 \sin^2 \theta^*} \\ &\times \left[1 - \cos \left(\frac{(\mathbf{q}_1^2 - 2\omega \sin \theta^* \mathbf{q}_1 \cdot \hat{\delta} + \omega^2 \sin^2 \theta^*) \Delta z}{2\omega} \right) \right].\end{aligned}\quad (7)$$

In Eq. (7) the two terms, $|\mathcal{M}_a|^2$ and $2\text{Re}\mathcal{M}_b^\dagger \mathcal{M}_c$ are individually divergent. Their sum is, however, well defined due to the cancellation of the soft and collinear singularities. From Eq. (7) the gluon distribution is not only finite when $\theta^* \rightarrow 0$ but vanishes on average due to the uniform angular distribution of momentum transfers from the medium, $\int_0^{2\pi} d\alpha \cos \alpha = 0$. Here $\cos \alpha = \mathbf{q}_1 \cdot \hat{\delta}/|\mathbf{q}_1|$. We have checked that for physical gluons of $|\mathbf{k}| \leq \omega$ the cancellations

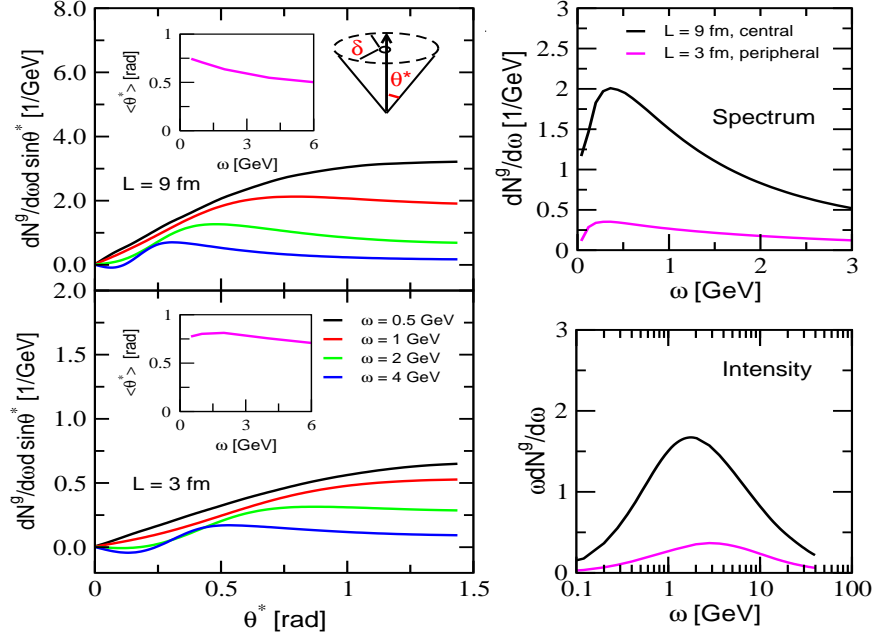


Figure 2. The angular distribution of medium-induced bremsstrahlung of $E = 6$ GeV gluon jet for fixed values of the radiative gluon energy $\omega = 0.5, 1, 2, 4$ GeV. Top and bottom panels represent (1+1)D Bjorken expanding medium of transverse size $L = 9$ fm and $L = 3$ fm, respectively. Inserts show $\langle\theta^*\rangle$ versus ω . Right panels illustrate the gluon spectrum and radiation intensity of $E = 40$ GeV gluon jet.

discussed here persist to all orders in the mean number of scatterings [8]. The small frequency and small angle spectral behavior of $dN_{\text{med}}^g/d\omega d\sin\theta^* d\delta$ remains under perturbative control.

We also emphasize that destructive quantum interference suppresses radiation of $\Delta z \ll l_f$ [8]. Gluons of final transverse momentum \mathbf{k} are initially much more collinear with the jet but acquire their moderately large angle θ^* from momentum transfers from the medium. The formation length at the emission vertex, which allows for interference on the scale of the nuclear size, reads

$$l_f = \frac{2\omega}{(\mathbf{k} - \mathbf{q}_1)^2} = \frac{2\omega}{\mathbf{q}_1^2 - 2\omega \sin\theta^* \mathbf{q}_1 \cdot \hat{\delta} + \omega^2 \sin^2\theta^*}. \quad (8)$$

The induced radiation decouples from the jet at $l_f \sim \Delta z \propto L/2$ and reduces the possibility of gluon showering due to further interactions in the plasma. For example, in central $L = 9$ fm collisions $\langle l_f \rangle \simeq 4$ fm and with formation times $z_0 = 0.25 - 0.5$ fm by the time a physical gluon is formed the plasma density has dropped by a factor of 8 to 16 from the longitudinal Bjorken expansion.

Given the vastly different angular behavior of the vacuum and the medium-induced gluon bremsstrahlung, Eqs. (1) and (7), it is critical to identify the phase space where cancellation of the color currents induced by the hard and soft scattering occurs. We fix the parameters of the medium in Eq. (7) to $\mu(z_0) = 1.5$ GeV and $\lambda_g(z_0) = 0.75$ fm at initial formation time $z_0 = 0.25$ fm. Since small $|\mathbf{k}|$ and ω emission is suppressed, we use only a moderate $\alpha_s = 0.25$. Triggering on high p_{T_1} hadron directs its parent parton “c” away from the medium and places the collision point of the lowest order (LO) $ab \rightarrow cd$ underlying perturbative process [16] close to the periphery of the nuclear overlap region. Then, it is the back-scattered jet “d” that traverses the QGP. For large nuclei, such as Au and Pb, path lengths $L = 9$ (3) fm are used to

illustrate central (peripheral) collisions, respectively. We limit gluon emission to the forward jet hemisphere, $0 \leq \theta^* \leq \frac{\pi}{2}$.

The angular distribution of medium-induced radiation for $E = 6$ GeV gluon jet for select values of ω is shown in the right panels of Fig. 2. We find that gluon emission is strongly suppressed within a cone of opening angle $\theta^* \simeq 0.25$ rad due to the cancellation of collinear bremsstrahlung – a mechanism different from a Gaussian random walk in θ^* . The broad gluon distribution can be characterized by the mean emission angle

$$\langle \theta^* \rangle = \int_0^1 \theta^* \frac{dN_{\text{med}}^g}{d\omega d\sin\theta^*} d\sin\theta^* \left[\int_0^1 \frac{dN_{\text{med}}^g}{d\omega d\sin\theta^*} d\sin\theta^* \right]^{-1}, \quad (9)$$

given in the inserts of Fig. 2. Left panels illustrate the infrared safety property of the spectrum. Energy loss is dominated by semihard few GeV gluons, see $\omega dN^g/d\omega$. The gluon number $dN^g/d\omega$ distribution peaks at even smaller frequencies ω . Momentum transfers from the medium $|\mathbf{q}_1| \sim 1 - 2$ GeV are clearly able to generate broad angular bremsstrahlung distribution. However, it is the cancellation of the $\theta^* \rightarrow 0$ radiation together with the model of the medium which ensure the weak ω dependence of the mean emission angle $\langle \theta^* \rangle \sim 0.5$ rad seen in Fig. 2.

3. Suppression of the single inclusive hadrons

Dynamical nuclear effects in multi-particle production in A+B collisions can be studied through the ratio

$$R_{AB}^{(n)} = \frac{d\sigma_{AB}^{h_1 \dots h_n}/dy_1 \dots dy_n d^2p_{T_1} \dots d^2p_{T_n}}{\langle N_{AB}^{\text{coll}} \rangle d\sigma_{NN}^{h_1 \dots h_n}/dy_1 \dots dy_n d^2p_{T_1} \dots d^2p_{T_n}}. \quad (10)$$

In Eq. (10) $\langle N_{AB}^{\text{coll}} \rangle$ is the mean number of binary collisions which can be calculated from an optical Glauber model.

Results from the perturbative calculation of the nuclear modification to the neutral and charged pion production in central $Au + Au$ collisions are given in the left hand side of Figure 3. At all energies there is cancellation between the Cronin enhancement, which arises from the transverse momentum diffusion of fast partons in cold nuclear matter [5, 17, 18, 19], and the subsequent inelastic jet attenuation in the final state. This interplay is most pronounced at the low Super Proton Synchrotron (SPS) $\sqrt{s_{NN}} = 17$ GeV where, in the absence of quenching, the corresponding enhancement could reach a factor of 3-4 [5]. With final state energy loss taken into account, $R_{AA}^{h_1}(p_{T_1})$ is shown versus the WA98 [20] and the CERES [21] Pb+Pb and Pb+Au data with p+p baseline defined as in [22]. Systematic comparison of the calculated nuclear modification to the existing experimental measurements can also be found in [22]. The agreement between data and theory is good at high p_{T_1} but the quenching is over predicted at $p_{T_1} \sim \text{few GeV}$.

In two particle correlation measurements the energy loss of the second parent parton at high p_{T_1}, p_{T_2} qualitatively leads to $1 \leq R_{AA}^{h_1}/R_{AA}^{h_1 h_2} \leq 2$. Numerical estimates in Fig. 3(b) from jet quenching alone indicate that the double inclusive hadron suppression is 25% – 40% larger than the single inclusive quenching in the $5 \leq p_{T_1} = p_{T_2} \leq 7$ GeV range at $\sqrt{s_{NN}} = 62$ GeV. Double inclusive cross section quenching is manifest in the attenuation of the away-side correlation function $C_2(\Delta\phi) = (1/N_{\text{trig}})dN^{h_1 h_2}/d\Delta\phi$ [23]. In Fig 3(c) it leads to a 4 – 5 fold attenuation of the area A_{far} relative to the p+p case. In contrast, elastic transverse momentum diffusion will only result in a broader $C_2(\Delta\phi)$. We note that the experimentally measured suppression value will be sensitive to the subtraction of the elliptic flow v_2 component which may remove part or all of the residual correlations.

To study the details of non-Abelian energy loss in the QGP we extend the calculation of the quenching of the away-side di-hadrons to low values of p_{T_2} in the next section.

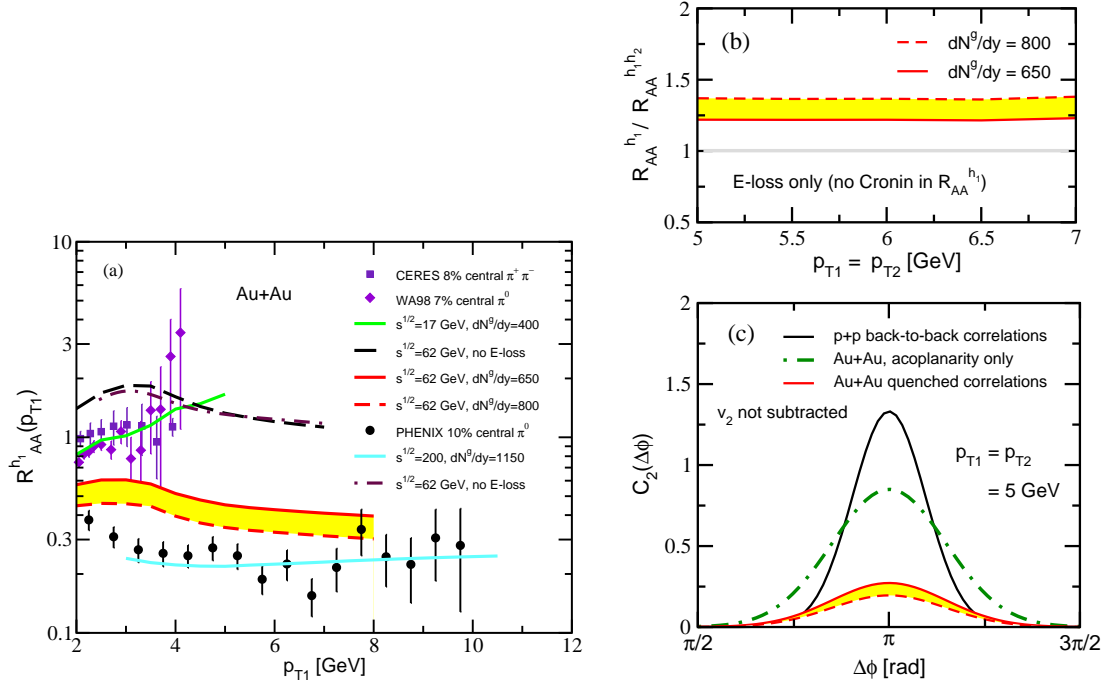


Figure 3. (a) Calculated nuclear modification factor $R_{AA}(p_{T1})$ versus the center of mass energy $\sqrt{s_{NN}} = 17, 62, 200$ GeV for central Au+Au collisions. The yellow band represents the perturbative QCD expectation for the depletion of the neutral pion multiplicity at $\sqrt{s_{NN}} = 62$ GeV. (b) The ratio of the attenuation of the single and double inclusive π^0 cross sections $R_{AA}^{h_1}(p_{T1})/R_{AA}^{h_1h_2}(p_{T1} = p_{T2})$ in central Au+Au collisions at $\sqrt{s_{NN}} = 62$ GeV and (c) the manifestation of the double inclusive hadron suppression in the quenching of the away-side di-hadron correlation function $C_2(\Delta\phi)$ [23].

4. Redistribution of the lost energy

Results reported in Ref. [12] are important for the future LHC heavy ion program since they for the first time suggest a large, and therefore detectable, broadening of the jet cone in the nuclear environment. Note that $\langle\theta^*\rangle$ implies a redistribution of the energy flow even within jets of large opening angle $R = \sqrt{\Delta\eta^2 + \Delta\phi^2} = 1$. If high statistics measurements of jet quenching away from midrapidity become available at RHIC II novel “octupol twist” moments of the parton absorption pattern in the QGP may be accessible [26]. At present, however, a key question for perturbative QCD phenomenology is whether the medium induced gluon bremsstrahlung can significantly alter the di-hadron correlations measured at midrapidity at RHIC [3, 4, 24, 25]. We naturally focus on the away-side $|\Delta\phi| \geq \frac{\pi}{2}$ case, where medium effects are the largest. Nuclear modifications build upon the LO double inclusive hadron production cross section, which is calculable in the perturbative QCD factorization approach [27] if either of the hadrons is moderately hard (p_{T1} or $p_{T2} \geq \text{few GeV}$) [16, 23]

$$\begin{aligned} \frac{d\sigma_{NN}^{h_1h_2}}{dy_1 dy_2 dp_{T1} dp_{T2} d\Delta\phi} &= K \sum_{abcd} \int_0^1 \frac{dz_1}{z_1} D_{h_1/c}(z_1) \left[D_{h_2/d}(z_2) \delta(\Delta\phi - \pi) \right] \frac{\phi_{a/N}(x_a) \phi_{b/N}(x_b)}{x_a x_b S^2} \\ &\times 2\pi\alpha_s^2 |\overline{M}_{ab \rightarrow cd}|^2. \end{aligned} \quad (11)$$

In Eq. (11) $K = 2$ is a next-to-leading order K -factor, $x_{a,b} = p_{a,b}/p_{N_a, N_b}$ are the momentum fractions of the incoming partons and $z_{1,2} = p_{h_1, h_2}/p_{c, d}$ are the momentum fractions of the

hadronic fragments. We use standard lowest order Gluck-Reya-Vogt PDFs [28] and Binnewies-Kniehl-Kramer FFs [29]. Renormalization, factorization and fragmentation scales are suppressed everywhere for clarity. The spin (polarization) and color averaged matrix elements $|\overline{M}_{ab \rightarrow cd}|^2$ are given in [16].

We first recall the physical effects that alter the LO perturbative formula, Eq. (11). A modification that does not change the $\Delta\varphi$ -integrated cross section is vacuum- and medium-induced acoplanarity [18, 24]. The deviation of jets from being back-to-back in a plane perpendicular to the collision axis arises from the soft gluon radiation and transverse momentum diffusion in dense nuclear matter [18]. In the approximation of collinear fragmentation, the width of the away-side hadron-hadron correlation function can be related to the accumulated di-jet transverse momentum squared in the φ -plane, $\sin \sqrt{\frac{2}{\pi}} \sigma_{\text{Far}} = \sqrt{\frac{2}{\pi} \langle k_T^2 \rangle_\varphi} / p_{\perp d}$. Assuming a Gaussian form,

$$f_{\text{vac. or med.}}(\Delta\varphi) = \frac{1}{\sqrt{2\pi}\sigma_{\text{Far}}} \exp \left[-\frac{(\Delta\varphi - \pi)^2}{2\sigma_{\text{Far}}^2} \right], \quad (12)$$

a good description of $|\Delta\varphi| \geq \frac{\pi}{2}$ correlations measured in elementary p+p collisions at $\sqrt{S} = 200$ GeV [7] requires a large $\langle k_{T \text{ vac}}^2 \rangle_\varphi = 5 \text{ GeV}^2$ for the di-jet pair with away-side scattered quark (and a 2.25 larger value for a scattered gluon). Additional broadening arises from the interactions of the jet in the QGP that ultimately lead to the reported energy loss. Using the parameters of the medium for (1+1)D expansion we find

$$\langle k_{T \text{ hot}}^2 \rangle = \int_{z_0}^L dz \, 2 \frac{\mu_D^2(z)}{\lambda_{q,g}(z)} = 2 \frac{\mu_D^2(z_0)}{\lambda_{q,g}(z_0)} \ln \frac{L}{z_0}, \quad (13)$$

although only half is projected on the φ -plane, $\langle k_T^2 \rangle_\varphi = \langle k_{T \text{ vac}}^2 \rangle_\varphi + \frac{1}{2} \langle k_{T \text{ hot}}^2 \rangle$.

Two competing mechanisms do, however, change the p_{T_2} dependence of the perturbative cross section, Eq. (11). First is the the parent jet “d” fractional energy loss $\epsilon = \Delta E_d / E_d$, which we here for simplicity consider on average and evaluate by integrating Eq. (7). It leads to a rescaling of the hadronic fragmentation momentum fraction $z_2 \rightarrow z_2 / (1 - \epsilon)$ [5]. Physically, fewer high p_{T_2} particles are produced by the attenuated parton of energy $E_d - \Delta E_d$. If the energy loss is large, a second mechanism is invoked as a consequence. Hadronic fragments of the radiative gluons will increase the probability of finding low and moderate p_{T_2} particles associated with the interacting jet [9].

To calculate di-hadron correlations, we first map the jet structure of a hard 90° -scattered parton on rapidity $y \approx \eta = -\ln \tan(\theta/2)$ (θ being the angle relative to the beam axis) and azimuth ϕ , $\tan^2 \theta^* = \cot^2 \theta + \tan^2 \phi$, $\tan \delta = -\cot \theta / \tan \phi$. The approximately flat rapidity distribution of the away-side jet near $y_2 = 0$ can be used to sum over all emission angles $\theta \in (\theta_{\min}, \theta_{\max}) \subset (0, \pi)$ yielding

$$\frac{dN_{\text{med}}^g}{d\omega d\phi} = \int_{\theta_{\min}}^{\theta_{\max}} d\theta \left[\frac{dN_{\text{med}}^g}{d\omega d \sin \theta^* d\delta} \left| \frac{\partial(\sin \theta^*, \delta)}{\partial(\theta, \phi)} \right| \right]. \quad (14)$$

The Jacobian of the transformation in Eq. (14) reads

$$\left| \frac{\partial(\sin \theta^*, \delta)}{\partial(\theta, \phi)} \right| = \frac{1}{\sin^2 \theta \cos^2 \phi} \frac{(\tan^2 \phi + \cot^2 \theta)^{-1/2}}{(1 + \tan^2 \phi + \cot^2 \theta)^{3/2}}. \quad (15)$$

It is critical to note that projection on a plane coincident with the jet cone axis (the ϕ -plane in Eq. (14) is one example) efficiently masks the $\theta^* \rightarrow 0$ void in the angular distribution of medium-induced gluons reported in Fig. 2. While projecting the medium induced radiation on the $y = 0$

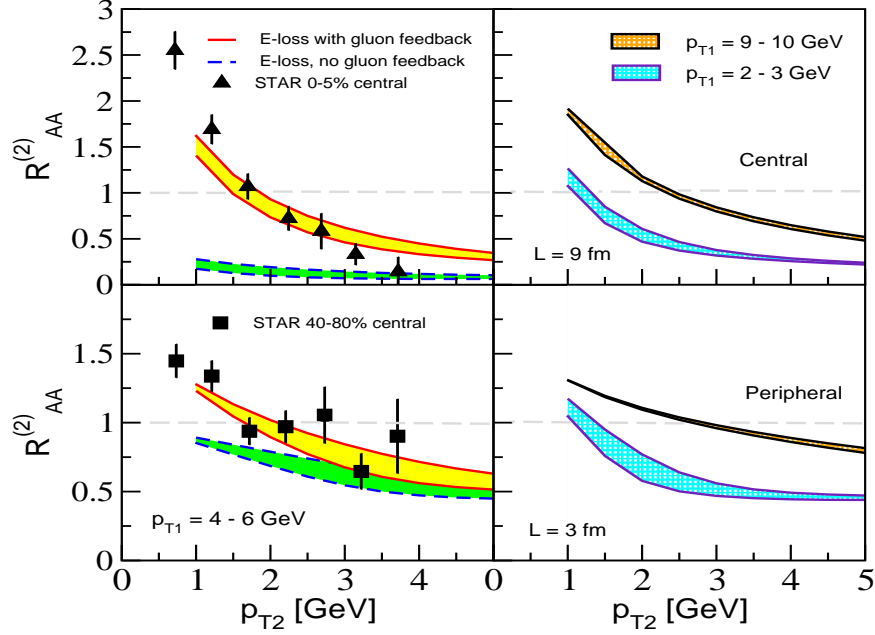


Figure 4. Nuclear modification of the back-to-back di-hadron correlations with and without the contribution of medium-induced bremsstrahlung. Top and bottom panels illustrate central and peripheral collisions, respectively. Data is from STAR [4]. Right panels predict $R_{AA}^{(2)}$ for low and high p_{T1} hadron triggers.

plane is an approximation with the largest deviations being close to the edges of phase space (in this case $\frac{\pi}{2}$ and $\frac{3\pi}{2}$), it is much less expensive computationally than a full simulation of the away-side jet+gluons. Our conclusion about the importance of the broad rapidity distribution of di-jets and the vacuum and medium-induced acoplanarity is independent of the physical mechanism that depletes the parton (or particle) multiplicity in a cone around the jet axis.

The end analytic result for the modification to Eq. (11) per average nucleon-nucleon collision in the heavy ion environment can be derived from the energy sum rule for all hadronic fragments from the jet,

$$\begin{aligned}
 D_{h2/d}(z_2)\delta(\Delta\varphi - \pi) &\Rightarrow \frac{1}{1-\epsilon} D_{h2/d}\left(\frac{z_2}{1-\epsilon}\right) f_{\text{med.}}(\Delta\varphi) + \frac{p_{T1}}{z_1} \int_0^1 \frac{dz_g}{z_g} D_{h2/g}(z_g) \\
 &\times \int_{-\pi/2}^{\pi/2} d\phi \frac{dN_{\text{med}}^g(\phi)}{d\omega d\phi} f_{\text{vac.}}(\Delta\varphi - \phi) .
 \end{aligned} \tag{16}$$

Here, $z_g = p_{T2}/\omega$.

Whether medium-induced gluon radiation may have significant observable consequences for the large angle di-hadron correlations depends on its relative contribution to the $\Delta\varphi$ -integrated cross section. From Eq. (11) this can be studied versus p_{T2} via the ratio $R_{AA}^{(2)}$ [23]. Numerical results, shown in Fig. 4, correspond to triggering on a high $p_{T1} = 4 - 6$ GeV pion and measuring all associated $\pi^+ + \pi^0 + \pi^-$. Depletion of hadrons from the quenched parent parton alone leads to a large suppression of the double inclusive cross section with weak p_{T2} dependence. Hadronic feedback from the medium-induced gluon radiation, however, completely changes the nuclear modification factor $R_{AA}^{(2)}$. It now shows a clear transition from a quenching of the away-side jet at high transverse momenta to enhancement at $p_{T2} \leq 2$ GeV, a scale significantly larger

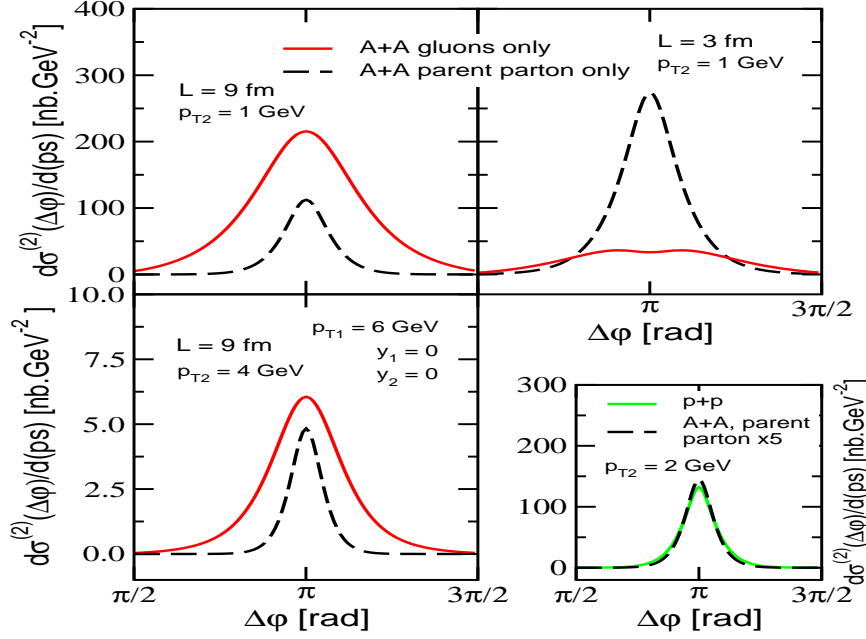


Figure 5. The angular distribution of $|\Delta\phi| \geq \frac{\pi}{2}$ di-hadrons for central and peripheral A+A collisions. Solid and dashed lines give *separately* the contribution of the radiative gluons and the attenuated parent parton. The lower right panel compares the the width of the correlation function in p+p to the one of the suppressed parent parton in central A+A reactions.

than the one found in [9]. In fact, we have checked that for large ΔE_d the back-to-back di-hadron correlations are dominated by radiative gluons to unexpectedly high $p_{T_2} \sim 10$ GeV. It should be noted that the experimental trigger introduces a bias toward large z_1 , which is difficult to account for analytically. Therefore we expect deviations between theory and the measurement when $p_{T_2} \geq p_{T_1}$. STAR data in central and peripheral Au+Au collisions [4] is shown for comparison. Experimentally testable predictions for the shape and magnitude of $R_{AA}^{(2)}$ and the enhancement-to-suppression transition $R_{AA}^{(2)} = 1$ versus p_{T_1} are also given in Fig. 4. It has been previously argued [30] that detailed balance reduces jet suppression at partonic scales $p_{\perp_d} \leq \text{few } \mu_D$, though such mechanism cannot produce enhancement of the low transverse momentum particle production observed in Fig. 4.

With a dominant contribution to the di-hadron yields, the medium induced gluons are bound to also determine the width of the correlation function. Two-particle distributions in A+A reactions, calculated from Eqs. (11) and (16) for a $p_{T_1} = 6$ GeV trigger pion and two different $p_{T_2} = 1, 4$ GeV associated pions, are shown in Fig. (5). Qualitatively, the medium-induced gluon component to the cross section controls the growth of the correlation width in central and semi-central nuclear collisions. Quantitatively, the effect should be even larger than the one estimated here, which is limited by the imposed $0 < \theta^* < \frac{\pi}{2}$ constraint. The decisive role of the bremsstrahlung spectrum, Eq. (7), in establishing the $\Delta\phi$ -shape of away-side di-hadrons is further clarified in the bottom right panel of Fig. 5. Hadronic fragments from the quenched parton “d” *only* are shown to yield a distribution that is *not* broader than the one anticipated in p+p reactions. Experimental measurements of significantly enhanced widths for $|\Delta\phi| \geq \frac{\pi}{2}$ two-particle correlation in A+A collisions should thus point to copious hadron production from medium-induced large angle gluon emission.

5. Conclusions

In summary, we calculated the transverse momentum and angular distribution of the away-side di-hadron correlations in the framework of the perturbative QCD factorization approach, augmented by inelastic jet interactions in the quark-gluon plasma. At RHIC energies we found that the medium-induced gluon radiation determines the two-particle yields and the width of their correlation function to surprisingly high transverse momentum $p_{T_2} \sim 10$ GeV. Clear transition from back-to-back jet enhancement to back-to-back jet quenching is established at moderate $p_{T_2} = 1 - 3$ GeV, independent of collision centrality but sensitive to the trigger hadron momentum p_{T_1} . Definitive experimental determination of its features, predicted in Ref. [12], will for the first time provide a handle on the *differential spectrum* of medium-induced non-Abelian bremsstrahlung. Coincidental confirmation of large broadening of the away-side di-hadrons would require a critical reassessment of the origin of intermediate transverse momentum particles in central and semi-central nuclear collisions. A full numerical simulation of jets away from midrapidity is required for more quantitative studies of the two particle topology. For jet physics at the LHC, our findings ensure a measurable increase in the jet width in ultradense nuclear matter.

Acknowledgments

This work is supported by the J. Robert Oppenheimer Fellowship of the Los Alamos National Laboratory and by the US Department of Energy.

References

- [1] P. Levai *et al.*, Nucl. Phys. A **698**, 631 (2002); K. Adcox *et al.*, Phys. Rev. Lett. **88**, 022301 (2002).
- [2] S. S. Adler *et al.*, Phys. Rev. Lett. **91**, 072301 (2003).
- [3] C. Adler *et al.*, Phys. Rev. Lett. **90**, 082302 (2003).
- [4] J. Adams *et al.*, nucl-ex/0501016; F. Wang, J. Phys. G **30**, S1299 (2004).
- [5] M. Gyulassy, I. Vitev, X. N. Wang, Phys. Rev. Lett. **86**, 2537 (2001). I. Vitev, M. Gyulassy, Phys. Rev. Lett. **89**, 252301 (2002).
- [6] X. N. Wang, Phys. Lett. B **595**, 165 (2004).
- [7] J. Adams *et al.*, Phys. Rev. Lett. **91**, 072304 (2003).
- [8] M. Gyulassy, P. Levai, I. Vitev, Phys. Rev. Lett. **85**, 5535 (2000); Nucl. Phys. B **594**, 371 (2001); Nucl. Phys. B **571**, 197 (2000).
- [9] S. Pal, S. Pratt, Phys. Lett. B **574**, 21 (2003).
- [10] R. Baier *et al.*, Phys. Rev. C **60**, 064902 (1999).
- [11] C. A. Salgado, U. A. Wiedemann, Phys. Rev. Lett. **93**, 042301 (2004).
- [12] I. Vitev, hep-ph/0501255.
- [13] T. Kinoshita, J. Math. Phys. **3**, 650 (1962); T. D. Lee, M. Nauenberg, Phys. Rev. **133**, B1549 (1964).
- [14] L. D. Landau and I. Pomeranchuk, Dokl. Akad. Nauk Ser. Fiz. **92**, 535 (1953); A. B. Migdal, Phys. Rev. **103**, 1811 (1956).
- [15] M. Djordjevic and M. Gyulassy, Nucl. Phys. A **733**, 265 (2004); Phys. Lett. B **560**, 37 (2003).
- [16] J. F. Owens, Rev. Mod. Phys. **59**, 465 (1987).
- [17] I. Vitev, Phys. Lett. B **562**, 36 (2003).
- [18] J. W. Qiu and I. Vitev, Phys. Lett. B **570**, 161 (2003); M. Gyulassy, P. Levai and I. Vitev, Phys. Rev. D **66**, 014005 (2002).
- [19] Y. Zhang, G. I. Fai, G. Papp, G. G. Barnafoldi and P. Levai, Phys. Rev. C **65**, 034903 (2002).
- [20] M. M. Aggarwal *et al.*, Eur. Phys. J. C **23**, 225 (2002).
- [21] G. Agakishiev *et al.*, hep-ex/0003012.
- [22] D. d'Enterria, Phys. Lett. B **596**, 32 (2004); J. Phys. G **31**, S491 (2005); nucl-ex/0504001.
- [23] J. W. Qiu, I. Vitev, hep-ph/0405068.
- [24] J. Rak, J. Phys. G **30**, S1309 (2004); J. Phys. G **31**, S541 (2005).
- [25] K. Filimonov, J. Phys. G **31**, S513 (2005).
- [26] A. Adil and M. Gyulassy, nucl-th/0505004.
- [27] J. C. Collins, D. E. Soper, G. Sterman, Nucl. Phys. B **261**, 104 (1985).
- [28] M. Gluck, E. Reya, A. Vogt, Eur. Phys. J. C **5**, 461 (1998).
- [29] J. Binnewies, B. A. Kniehl, G. Kramer, Z. Phys. C **65**, 471 (1995).
- [30] E. Wang, X. N. Wang, Phys. Rev. Lett. **87**, 142301 (2001).